



# The Impact of Range and Incident Angle Variation on Surface Reflectivity and Roughness-Based TLS Point Cloud Accuracy

Bakhtyar Ahmed Mala <sup>1,2</sup> \* , and Dleen Muhammed Salih <sup>2</sup> 

<sup>1</sup> Survey and Geomatics, College of Engineering, Tishk International University, Erbil, Iraq

<sup>2</sup> Geomatics, College of Engineering, Salahaddin University, Erbil, Iraq.

## Article History

Received: 10.06.2024

Revised: 19.08.2024

Accepted: 27.08.2024

Published: 01.09.2024

Communicated by: Dr. Orhan Tug.

\*Email address:

[bakhtyar.mala@su.edu.krd](mailto:bakhtyar.mala@su.edu.krd)

\*Corresponding Author



Copyright: © 2023 by the author.  
Licensee Tishk International University,  
Erbil, Iraq. This article is an open-access  
article distributed under the terms and  
conditions of the Creative Commons  
Attribution-Noncommercial 2.0 Generic  
License (CC BY-NC 2.0)  
<https://creativecommons.org/licenses/by-nc/2.0/>

## Abstract:

TLS has intriguing experimental procedures to investigate how various scanned surface reflectivity and roughness affected the accuracy of the scanned TLS data at various incident angles and ranges. Thus, different materials (glass, steel, wood, Ekoplast, and the sheet target of the total station) were used. During the experiment, four distinct ranges (5 m, 20 m, 40 m, and 60 m) under the same weather conditions were employed. The selected materials were scanned at 6 incident angles from 0° to 75°, rotating 15° per scan. This means a total of 96 scans were measured. At various scan angles and ranges, smooth surfaces have a greater effect on the quality of the scanned data than rough surfaces. The whole Total Station (TS) target reflects approximately 200mm closer to the instrument at 0° incident angle than the other materials at the 5m range; this difference decreases as the incident angle increases. On the other hand, this difference also decreases with increasing the range; at 0° and 5m range, it's about 200mm, while for the same angle and 60m range, it's about 120mm. Furthermore, the density of the point clouds decreases with increasing range. Finally, the effect of the distance clearly appeared on the small incident angle rather than the large incident angle.

**Keywords:** Laser Scanner; Incident Angle; Range; Different Materials; Roughness; and Reflectivity

## 1. Introduction

There are numerous strategies that differ between conventional and modern procedures in order to create an accurate model of expensive things such as heritages, oil tanks, and statues. Using a sensor and camera, laser-based and image-based techniques are the most modern and new methods [1]. The most precise and modern method in this sector is called terrestrial laser scanning (TLS).

In essence, two-way journey periods (time of flight) are used by laser scanner systems to calculate the distance ( $\rho$ ) between the instrument and the items being scanned. It is not necessary to fix the targets on the scanned items' material surfaces; reflector-less scanner systems are typically preferred in the scanning procedure. The range is determined by how much of the returned signal reaches the scanner's object (photodetector). In order for the laser beam's footprint area and amount of received signal by the scanning range finder to be affected by its trip time,

The intensity of returned back signals from the object's surface to the instrument (the scanner) is not equal for the same material or color at the same time of scanning and range, based on the experimental tests. Many factors affected the returned laser beam, such as incident angle, range, sunshine, material properties, and surface type. The scanner measures the reflected laser beams from the material by measuring the reflected light path and retracing the path of the traveled laser path.

The value of the incident angle always varies between zero and 90 degrees. A laser beam hitting the surface perpendicularly results in a circular footprint on the surface of the objects. The size of the circular footprint increases with increasing range between the scanner and the scanned objects due to beam divergence and a weaker returned signal [2]. While the laser beam hits the surface with a non-zero incident angle, the resulting footprint of the surface is elongated; therefore, the energy distributed is also spread and forms an ellipse on the surface of the object [3].

This study focuses on performing different scans with particular properties for different material surfaces in different ranges and under the same atmospheric conditions. It seeks to investigate how scanning various surfaces, both in terms of roughness and smoothness, affects the precision and accuracy of the data at various incident scan angles and distances between the objects and TLS. The positional accuracy of the point clouds was found based on the best-fit patch creation for each surface and find the deviation of the point clouds from this created patch.

## 2. Literature Review

It's important to notice that a wide range of variables and material qualities, including measurement geometry, meteorological conditions, and equipment impacts, influenced the observed point clouds. Nonetheless, it was impacted by certain factors that were regarded as genuine issues, such as the instrument's geometry [4], the oscillating mirror problems [5], incident angle [6], beam divergence angle [6], the calibration process methods [7] and [8], and the type of instrument based on the manufacturer, such as Faro, Topcon, Leica, and Trimble.

On the other side, the majority of factors that affect the quality and accuracy measured by TLS point clouds are the scanning geometry, such as incident angle and distance [9], [10], and [6]. Obviously, scanning different kinds of objects provides different accuracies and qualities due to the color effects, material type, and quality of the surface [11], [12], and [13]. Despite the major effects of the incident angle and range on the quality of the measured point clouds, only a limited number of researchers have worked in this field, especially in terms of the position accuracy of the point clouds.

## 3. Material Preparations and Methodology

### 3.1 Select Materials

Regardless of whether the materials are natural or man-made, surface roughness and reflectivity are two main characteristics that could have a substantial impact on the precision of the scanned and measured data [14].

Four distinct materials were chosen for this study's technique, and they were all prepared for scanning. They used two primary criteria for their selection of materials: first, the most usable material found in man-made objects, including towers or skyscrapers. Second, there is a valuable difference in the reflectivity and surface roughness of the materials. For this reason, Ekoplast, wood, steel, and glass were the chosen materials. Each selected material has a surface roughness that varies significantly and is mostly employed in man-made construction.

The properties of the materials that were chosen were examined, and all necessary data was ascertained, including the material dimensions, which are as illustrated below: glass with a thickness of 6 mm and dimensions of 80 x 80 cm is used like a mackle to reflect the laser beam onto the scanner. Regarding steel, it is another material that is used in construction projects like buildings and bridges. The dimensions of Steel's sample are 80 x 80 cm with a thickness of 1.8 mm.

Furthermore, the majority of bookcases, doors, lockers, and constructions are made of wood. Its model had the same measurements 80 × 80 cm and a thickness of only 8 mm. It was constructed

completely of wood without any painting or covering. Finally, but just as importantly, EkoPlast is a material that is commonly used to plaster the exterior of a building to isolate and disperse heat, sound, and cold. These kinds of materials need to be mixed with water to make goods like stucco, parget, and gypsum. Additionally, it is equipped with a number of internal parts that filter both hot and cold air entering the building from the outside and vice versa. As a result, an EkoPlast with a 20 mm thickness and an 80 x 80 cm size dimension has been performed for this research.

Conversely, materials such as steel and glass are regarded as smooth surfaces based on the laser scanner beam's size, whereas materials such as wood and EkoPlast are regarded as rough surfaces based on the Bidirectional Reflectance Distribution Function (BRDF). Figure 1 shows all of the materials used in this research study.

Finally, five TS target sheets were positioned on each object surface to examine how the smoothest and most reflective surfaces affected the quality and accuracy of the data seen at different angles of scan and ranges. The kind of target for target scanning is a 4 x 4 cm reflective sheet target with a 1 mm thickness, approximately. These types of targets are flawlessly smooth and feature the highest reflectivity possible.

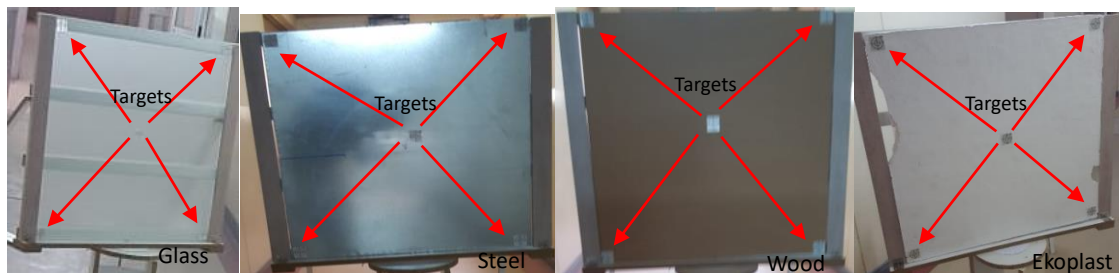


Figure 1: Selected materials utilized for the scanning operation

### 3.2 Stand Preparation

It is important to remember that precise and superior material sample scanning requires the construction of a stand. This is a result of the need to manage the scanning angle, maintain the material sample's vertical position during the measuring and scanning process, and establish the distance between the material sample and the scanner instrument as a scanned target. This platform was constructed out of wood since it was lightweight and reasonably priced, making it simple to transport from one place to another. In terms of layout and composition, it is divided into two separate sections: A sample of the material is placed inside and fastened using the first component (top), a frame measuring 1 x 0.8 m. Interestingly, this frame's design allows it to be easily removed from the structure body, making it simple and quick to replace or insert a sample of a different material. Regarding the lower section, there is a circular stand composed of wood, as seen in the middle of Figure 3. This component is 50 cm in height from the earth to the top of the structure. This section of the construction includes two circular bases, one up and one down. To create the verticality of the removable frame, there are two central holes at the exactly circular base's center, which lie on a single vertical line (see middle figure 3). Controlling this verticality was done with the centering laser beam of the Topcon TS equipment, as shown in Figure 3. Furthermore, the scan incident angles were controlled by a sharp fixed nail that was positioned near the upper circular portion's edge.



Figure 2: Utilizing the total station instrument's centering vertical laser beam to check the stand's verticality. The left image displays the controlling scan angle, the two right photos represent the verticality test, and the last is the TLS instrument used.

### 3.3 Methodology

The methodology for this study involved three main steps: the first step in adhering to the requirements for an accurate scanning process is selecting and preparing material samples that meet the required dimensions. Building the stand that is required to properly hold the material samples is another aspect of it. Setting the distance between the material stand and the scanning station, as well as configuring the TLS, are the tasks of the second step. Step three should be carried out by scanning the material sample at different scan angles and ranges. After that, all of the scanned data was processed by licensed Cyclone software, which is a specific software used for analyzing TLS data. The flowchart in Figure 2 below illustrates how the goals of this research were achieved.

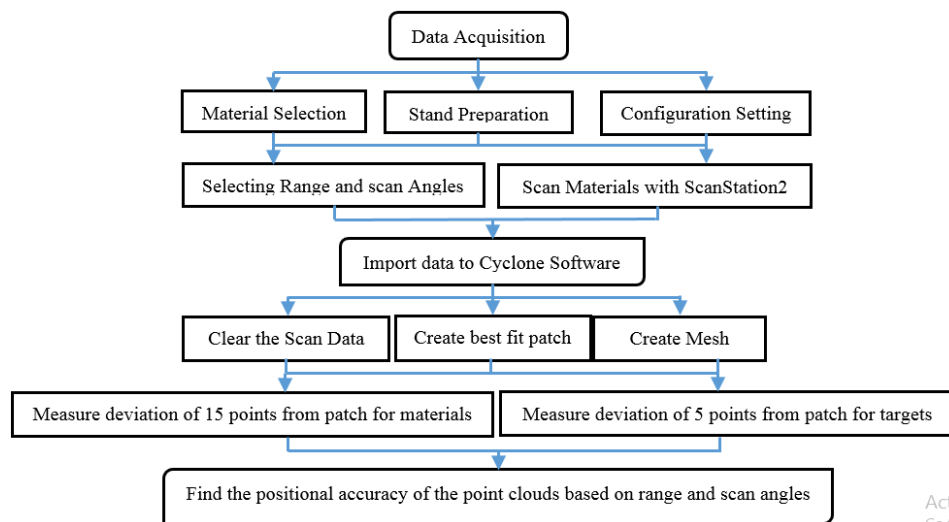


Figure 3: A diagram illustrates how data is measured and analyzed.

### 3.4 Scanning the materials

Samples of all prepared, chosen materials were measured and scanned at 6 different scan angles, like  $75^\circ$ ,  $60^\circ$ ,  $45^\circ$ ,  $30^\circ$ ,  $15^\circ$ , and  $0^\circ$ , and there were four distinct distances (about 5m, 20m, 40m, and 60m) between the scanner and the material's surface inside the stand. Thus, a total of 96 scans were carried out. Figure 4 provides some scanned data examples.



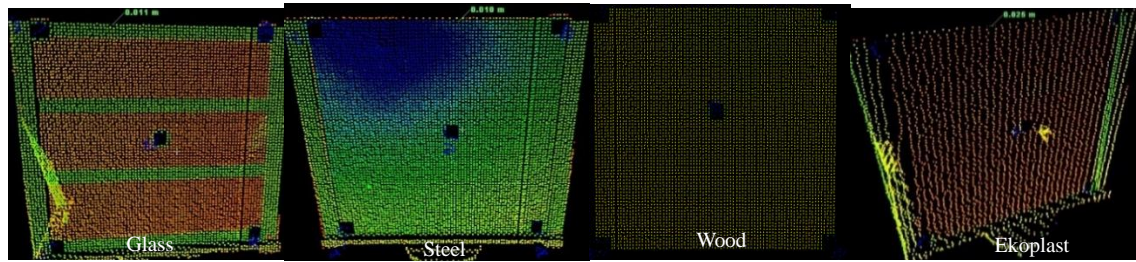


Figure 4: Glass, steel, wood, and Ekoplast are scanned surfaces, arranged from left to right at 5 m range and zero-degree scan angle

The ScanStation2 TLS equipment, whose specifications are shown in Table 1 below, was used for the scanning operations. Furthermore, the scanned data was stored and analyzed using Leica licensed cyclone software, which was directly connected to the PC via an Ethernet cable.

Table 1: Specifications of the ScanStation2 TLS

Name	Specification
Instrument type	Leica Geosystem, ScanStation2, laser class R3
Scanner Field of view	H., V. angles are: 360°, and 270°, respectively
2 Scanning windows	First window: -45 degrees to 32 degrees and Second window: 23.5° to 90°
Beam divergence	After 20 meters starts
Diameter of the beam	2.13mm
Scanning model	Pulse-based
Single-point cloud accuracy	4mm distance and position 6mm
Maximum distance	300 meters
Scanning rates	Up to 50000 pts/sec.

Interestingly, to investigate the impact of the smoothest and most reflective surface materials on the quality and accuracy of measured data (point clouds) at various scan angles, five adhesive TS targets were positioned at the center and corners of the scanned surface material's sample.

#### 4. Results

TLS is an instrument that has been used recently in various industries, including building, calibration, inspection, documentation, monitoring, and oil tank maintenance, among many other fields, because of its high level of precision while scanning objects. Like other devices, it is not exempt from noises occurring in the data that is measured. Therefore, to investigate the extent of their impacts on the accuracy and quality of the measured data, four different surface materials in terms of roughness and reflectivity were scanned at varying scan angles and ranges.

As previously noted, samples of selected materials, including glass, steel, wood, and Ekoplast, were used to conduct experimental tests. It is noteworthy to emphasize that the quantity of reflected point clouds varies depending on the properties, roughness, range, and heat of each substance. For instance, because of the substantial difference in surface roughness between the two materials, there were fewer reflected points from the glass surface material than from the wood at the same scan angle and range. As demonstrated in Figure 5, it is also evident that when the scan angle increases, the accuracy and quantity of reflected data (point clouds) from materials such as steel and glass drop significantly, and from materials such as wood and Ekoplast, they reduce gradually. On the other hand, given the same material and incidence angle, a greater range results in fewer point clouds. Consequently, the surface scan findings for each material are provided and analyzed individually

below, with the results demonstrating the simplicity of processing only the data for incident angles  $0^\circ$ ,  $30^\circ$ , and  $60^\circ$  we represented.

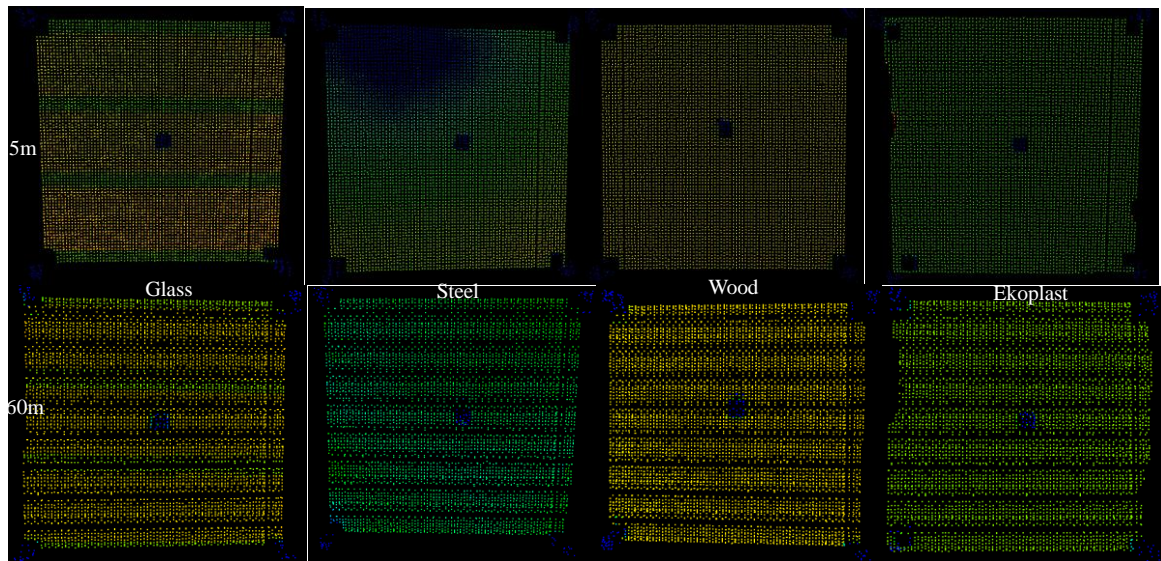


Figure 5: Glass, steel, wood, and ekoplast scanned material in (5 and 60) m ranges at  $0^\circ$  incidence angle.

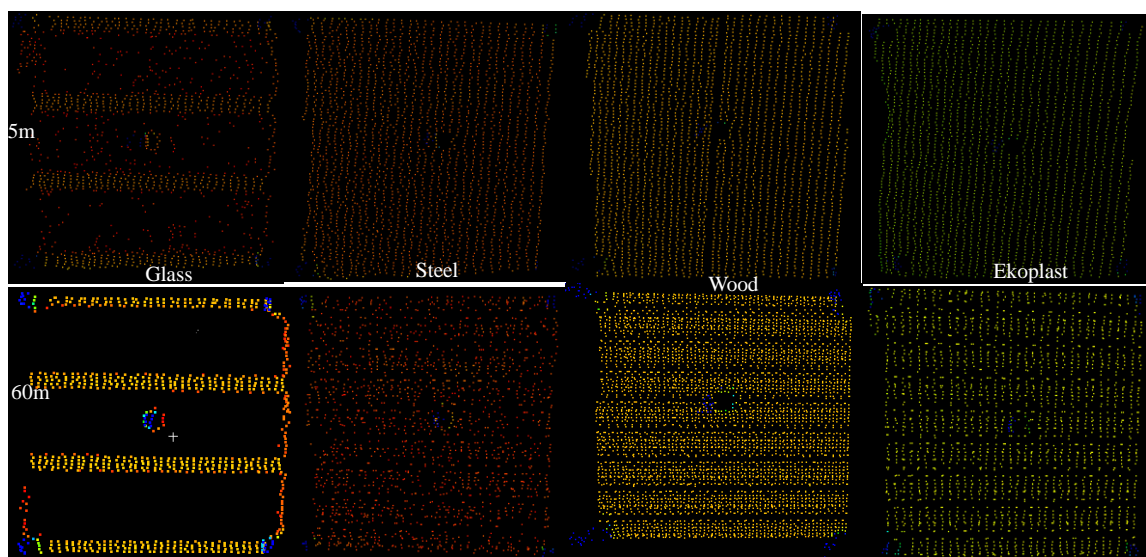


Figure 6: Glass, steel, wood, and ekoplast scanned materials at a  $60^\circ$  scan angle in the (5 and 60) m range.

Another factor that affects the accuracy and quality of the data (points) is the distance between the scanner and the scanned object. Before starting to scan the objects during the configuration setting, input the sample spacing between point clouds. For example, for all of the scanned objects and different distances, 1 cm of sample spacing was selected between two adjacent point clouds. This is performed to control and maintain the number of point clouds per unit area. However, many of the factors remain in the quality and accuracy of the data, such as the time of the scanned area increasing when the range between the scanner and objects increases. The other factor is that the beam divergence increases when the range increases, which means the footprint area per point cloud increases based on the range. Furthermore, during the travel of the laser beam in the atmosphere, for longer distances and times, the effect of the refraction and dust on the quality of the point clouds

increases compared to the short distances. Finally, the intensity of the returned signal decreases with increasing range based on the aforementioned factors.

#### 4.1 Glass Material Scanning Results

Typically, a regular mesh grid is made for the glass surface's gathered point clouds. In order to assess the degree to which the collected point data, in terms of densities, are placed on the same patched surface and the extent to which they are located far from it, a best-fit patch was created and performed on all of the scanned points on the surface of the glass, this process translated the accuracy and quality of the scanned data from the smooth surface of the glass. The primary goal of this study is to ascertain the accuracy and quality of the measured points. Consequently, range fluctuation has a greater impact on the density of accurately measured point clouds when scanning smooth materials like glass than it does on the precision and quality of measuring individual points. As the incidence angle increases, the density of point clouds rapidly drops. On the other hand, as range increases, so does the point cloud's density decrease, too. This is caused by a decrease in the projected scan surface (field of vision) and a decrease in the intensity of the returned signal as the incidence angle and range increase. Figure 7 illustrates that at a  $60^\circ$  incident angle (second row), the density data reflected from the surface of the glass decreased in comparison with the first row at a  $30^\circ$  incident angle. Furthermore, the density of the point clouds decreases with increasing range. In both rows, the range changes from left to right, specifically to 20 m, 40 m, and 60 m. It can also be easily seen that the intensity decreases for the same incident angle and different ranges.

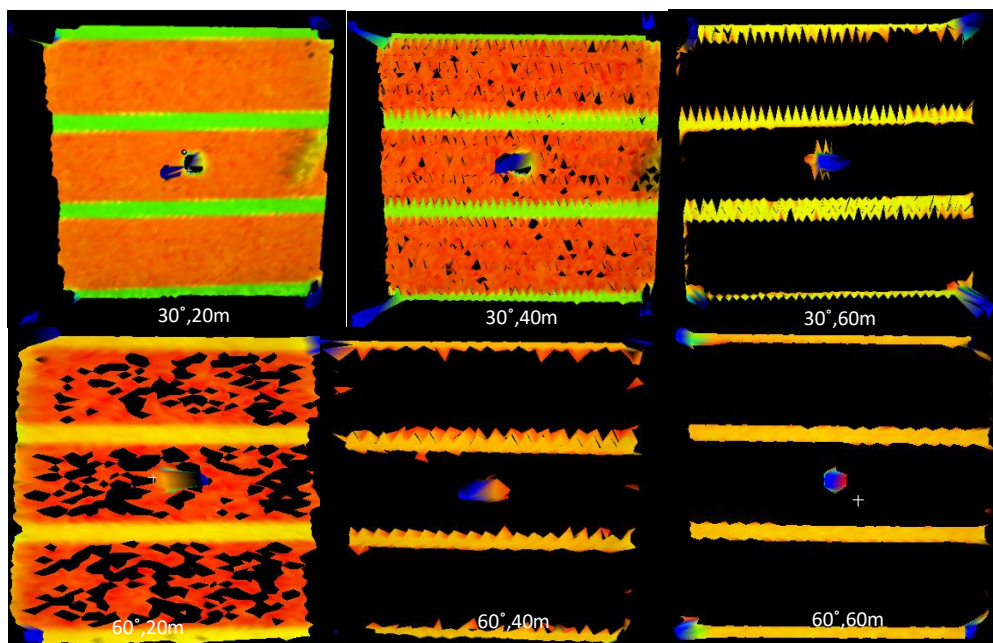


Figure 7: Meshed surfaces for glass material at  $30^\circ$  and  $60^\circ$  scan angles, in (20, 40, and 60) m ranges

Conversely, it becomes evident that the majority of the returned data appears as an image plane, like strips, when the best-fit patch is generated for the reflected signals. The fact that all of the gathered points on the strips are situated behind the best-fitted patch indicates that those points need additional time to travel before they can be detected by the scanner range finder. This occurs because a portion of the beam passes through the glass material and strikes the wood stand behind it, reflecting the light from the surface of the stand instead of the glass itself. It was quickly apparent that the majority of the reflected points, rather than coming from the glass surface itself, were actually returned from the wood object stand lines behind the glass Figure 8.



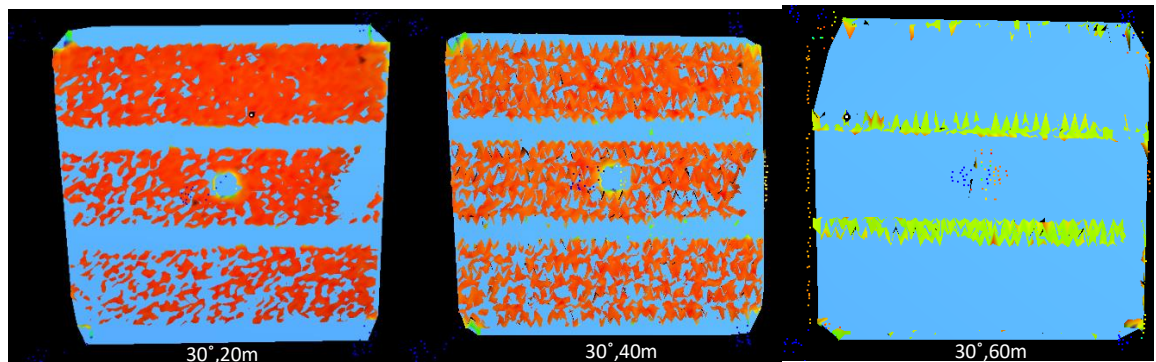


Figure 8: Producing mesh and fitted patch for points reflected from a glass at 30° scan angle and within a range of (20, 40, and 60) m.

A deviation value from the best-fit patch has been computed in the point cloud locations to investigate the impact of glass material on the accuracy of reflected data. As a result, 15 randomly chosen point clouds were dispersed around the surface, and 5 extra points were added to the TS target (an adhesive sheet) at every scan angle and range scan points from 0° to 75° and 5 to 60 meters. Figure 9 shows the outcome of the computed deviation for those 15-point clouds and the five-point clouds on the sheet targets.

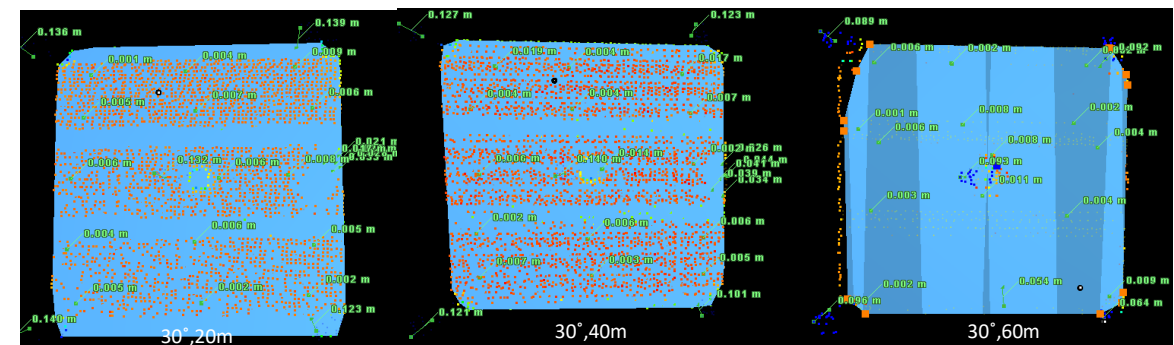


Figure 9: Selected 15 points plus 5 sheet points to examine the differences from the patch for glass material at: 30° scan angle and (20, 40, and 60) m ranges

Table 2: RMSE of 15 point clouds on glass material in 4 ranges and 3 incident angles

Degree s	5m	20m	40m	60m
Glass-0dg.	0.0029	0.0021	0.0019	0.0026
Glass-30dg.	0.0079	0.0051	0.0071	0.0047
Glass-60dg.	0.0048	0.0027	0.0025	0.0025

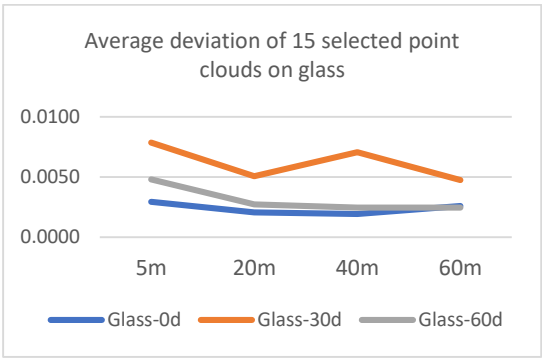


Figure 10: Graphical representation for an average deviation of 15 points on glass material in 4 ranges and 3 scan angles.

The departure of the average overall chosen point cloud data from the best-matched patch surface is shown in Figure 10 and Table 2. The overall deviation decreased for various scan angles, like 2 mm



in the 0° and 40 m ranges, while the highest deviation appeared at the 30° scan angle and 5 m range, nearing 8 mm.

The five sticky sheet targets were placed on the surface glass sample in different locations, parallel to the scanning glass, precisely in the middle, and on four of the corners. Each scanned target has several point clouds; to validate and find the deviation from the patch, only one point cloud was selected per target. The deviation findings of those spots progressively decrease as the impact angle rises from zero to 75 degrees, as shown in Table 3 and Figure 11. When the scan angle is 0° degrees, the deviation value is around 20 cm; at 60 degrees, the deviation value is approximately 2 cm. The effect of the distance on the deviation from the patch appeared on zero-degree incident angles more than on non-zero incident angles. When the range increases, the deviation from the patch decreases for the same incident angle. It can be easily seen at a zero-degree incident angle; it decreases from 19.32 cm to 12.62 cm because the intensity decreases, and then recognizing and detecting the properties of the surface materials decreases.

Table 3: Target RMSEs for 3 incident angles and 4 ranges on glass

Degrees	5m (m)	20m (m)	40m (m)	60m (m)
0dg.	0.1932	0.1942	0.1476	0.1262
30dg.	0.1268	0.1340	0.1224	0.0868
60dg.	0.0354	0.0368	0.038	0.0236

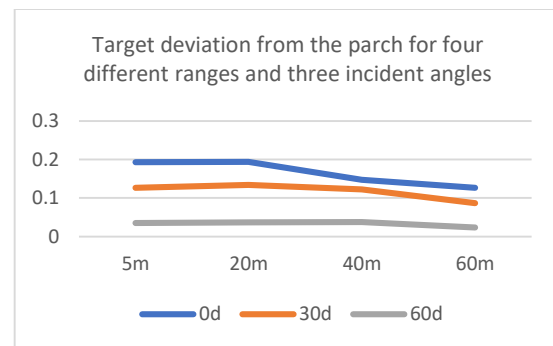


Figure 11: Graphical illustration of target deviation from the fitted patch for 3 scan angles and 4 ranges on glass material.

## 4.2 Steel Material Scanning Results

Steel is regarded as another substance with a smooth surface, similar to glass. The fluctuation in the incidence angle on smooth materials has a significant impact on the density and precision of single-point measurements of the reflected points. As the scanning angle increases, the density of point clouds decreases. Furthermore, the density of the point clouds decreases with increasing range. In both rows, the range changes from left to right, specifically to 20 m, 40 m, and 60 m. It is also easily noticeable that the intensity decreases for the same incident angle and different ranges. Then, a mesh grid is made for points see Figure 12.

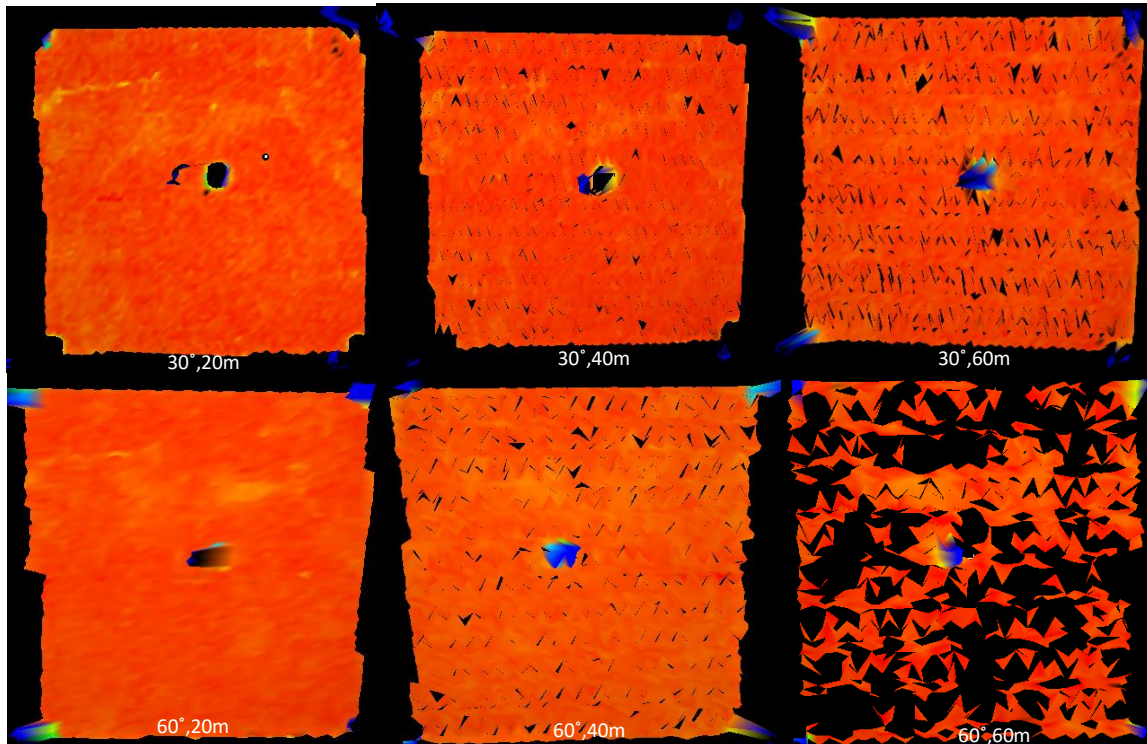


Figure 12: Steel meshed smooth surface material at (20, 40, and 60) m ranges and at 30° and 60° incident angles

After applying the best-fit patch for each scan, depending on the reflected point clouds, it is shown in Fig. 13 that the reflectivity of each point reflected from the steel surface varies with range. The point cloud departure from the patch for 30° at 20 m, 40 m, and 60 m ranges is clearly displayed in Figure 13.

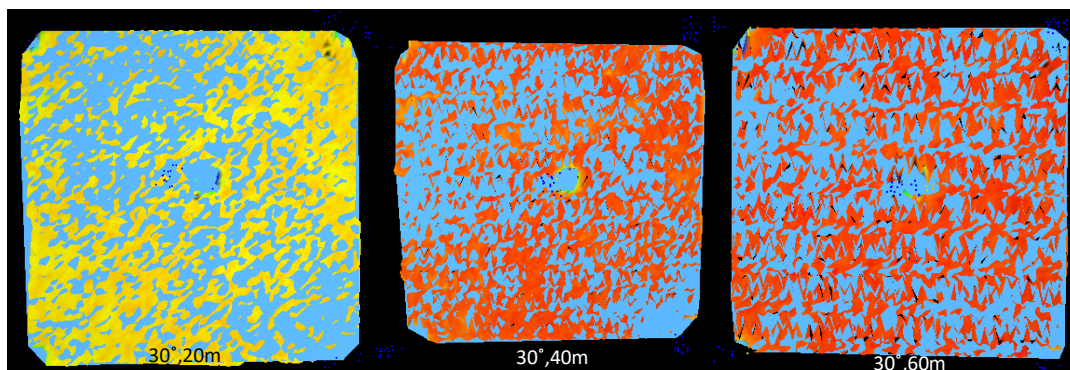


Figure 13: Create a mesh with the best-fit patch for the steel sample at a 30° scan angle and in the (20, 40, and 60) m range.

In order to evaluate the observed deviance from the fitted patch, a random selection of 15-point clouds was made, supplemented by 5 extra points on the sticky sheet total station target at every range and incidence angle scan data from 0 to 75 degrees. Figure 14 displays the calculated deviation's outcome.

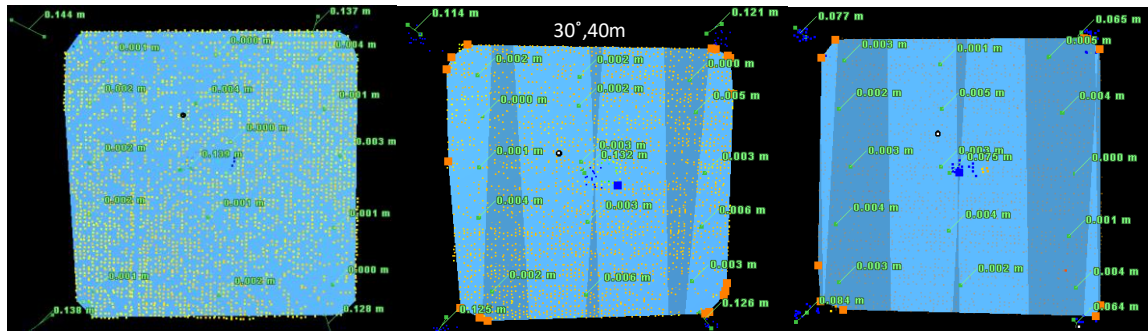


Figure 14: Selected 15 points plus 5 sheet points to examine the differences from the best patch of steel object at 30° scan angle and in (20, 40, and 60) m ranges.

Table 4: RMSE of 15 point clouds on steel material in 4 ranges and 3 incident angles

Degrees	5m (m)	20m (m)	40m (m)	60m (m)
Steel-0dg.	0.0021	0.0044	0.0019	0.0019
Steel-30dg.	0.0020	0.0016	0.0028	0.0029
Steel-60dg.	0.0018	0.0011	0.0019	0.0025

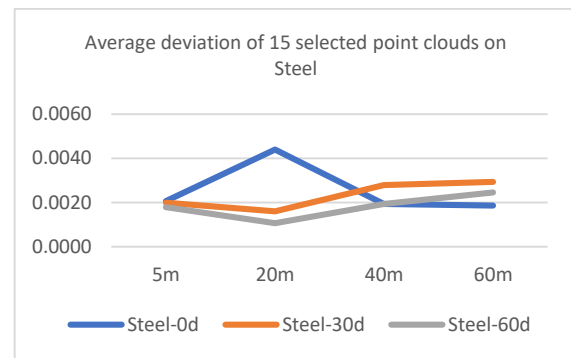


Figure 15: The graph shows an average deviation of 15 points on steel material at 4 ranges and 3 incident angles.

Figure 15 and Table 4 show the overall differences between the chosen points and the fitted patch. The maximum difference appeared in the 20-meter range at a scan angle near 5 mm. The zero incident angle is totally different from the non-zero incident angle in terms of changing deviation while increasing the range. At zero incident angle, from 5 m to 20 m, the deviation increases then decreases to 40 m and 60 m, but for non-zero incident angles, vice versa, because at zero incident angle, the steel was affected by the sun's shine in the 5 m and 20 m ranges.

Moreover, the steel surface has five fixed TS sheet targets fixed to it. For each target, a single point cloud is chosen in order to determine the deviation value from the fitted patch. The deviation values of the point clouds rapidly decrease at 0° to 60° incident angles, as Table 5 and Figure 16 demonstrate. The average overall deviation for the 5 and 20 m ranges was roughly 19 cm when the incident angle was equal to zero, and the deviation decreased as the range increased for the same incident angle. At 60 m, the deviation decreases to 11.5 cm for the same zero incident angle. While it is decreased to about 1.3 cm when the scan angle reaches 60° and 60m range. This indicates that when the incident angle and range rise, the intensity of the laser beam's returned signal decreases, making it impossible for the scanner to detect the impact of the material qualities.

Table 5: Target RMSEs for 3 different incident angles and 4 different ranges on steel

Degree s	5m (m)	20m (m)	40m (m)	60m (m)
0dg.	0.1888	0.1956	0.1476	0.1150
30dg.	0.1166	0.1372	0.1236	0.0730
60dg.	0.0152	0.0306	0.0302	0.0126

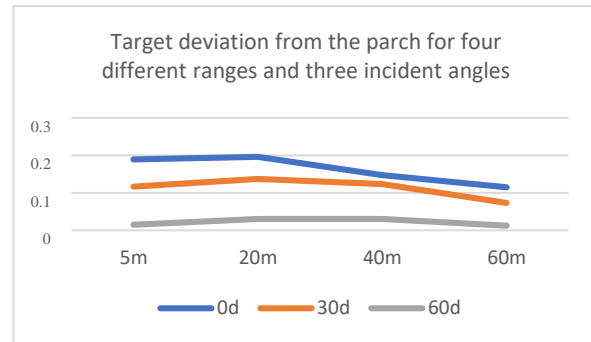


Figure 16: Illustration of target deviation from the fitted patch for 3 incident angles and 4 ranges on steel material.

It's interesting to note that, as Figure 17 illustrates, there was a serious issue when the deviation from the fitted patch was determined. This is the result of the sun's light striking the steel and glass surfaces at just the right angle relative to the scanner's incident angle. This causes the scanned laser beam to become more intense and causes the reflected points to return to the scanner sooner than other sections for the steel material, and the opposite is true for the glass material, where the sun's rays create a lens behind the glass surface. In Figure 18, the glass sample is scanned at a 30° incident angle in the 20m and 40m ranges, while the steel sample is scanned at a 0° incident angle in the 5m and 20m ranges. As can be observed, at a distance of between 5 and 40 meters from the scanner to the item on smooth surfaces, the sunlight effects are computed as a deviation value, or around 2 to 5 cm.

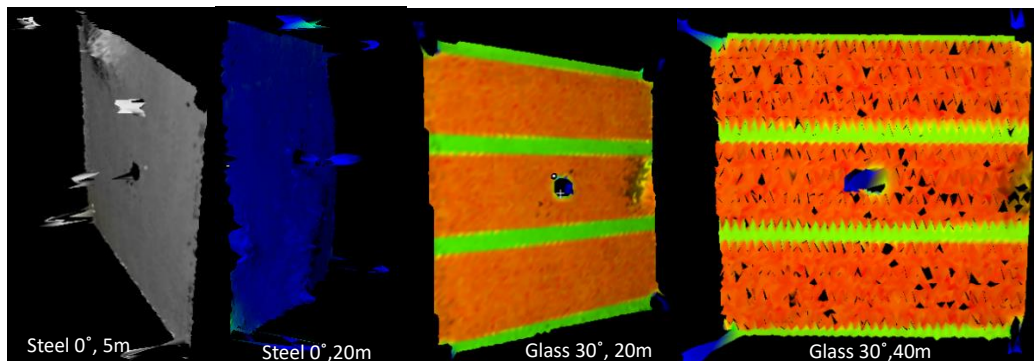


Figure 17: The drawback of smooth surfaces (glass and steel) when the sun shines coincides with the incident angle.



Table 6: The drawback of smooth surface materials (glass and steel) when the sun shines coincides with the incident angle.

Glass 20m- 30dg. (m)	Glass 40m- 30dg. (m)	Steel 5m- 0dg. (m)	Steel 20m- 0dg. (m)
0.0240	0.0360	0.0390	0.0300
0.0290	0.0330	0.0540	0.0380
0.0150	0.0310	0.0280	0.0270
0.0180	0.0210	0.0330	0.0370
0.0240	0.0280	0.0280	0.0290

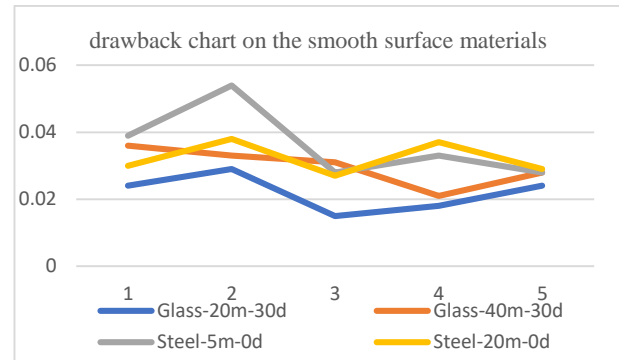


Figure 18: The drawback of smooth surfaces (glass and steel) when the sun shines coincides with the incident angle.

### 4.3 Wood Material Scanning Results

It's interesting to note that, as Figure 17 illustrates, there was a serious issue when the deviation from the fitted patch was determined. This is the result of the sun's light striking the steel and glass surfaces at just the right angle relative to the scanner's incident angle. This causes the scanned laser beam to become more intense and causes the reflected points to return to the scanner sooner than other sections for the steel material, and the opposite is true for the glass material, where the sun's rays create a lens behind the glass surface. In Figure 18, the glass sample is scanned at a 30° incident angle in the 20m and 40m ranges, while the steel sample is scanned at a 0° incident angle in the 5m and 20m ranges. As can be observed, at a distance of between 5 and 40 meters from the scanner to the item on smooth surfaces, the sunlight effects are computed as a deviation value, or around 2 to 5 cm.

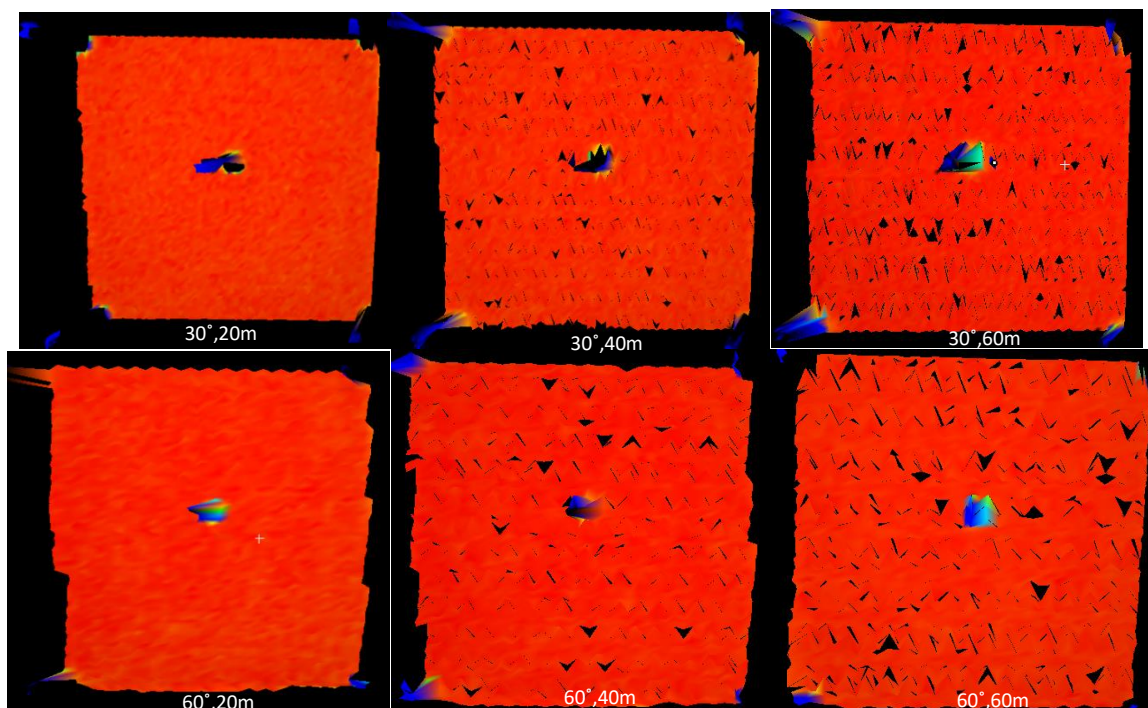


Figure 19: Meshed surface of wood rough surface in (20, 40, and 60) m ranges and at 30° and 60° incident angles.

All scans based on reflected point clouds had best-fit patches made for them as well since Figure 20 shows that the reflectance of each reflected point cloud from the wood surface varies with range and incidence angle change. Evidently, for a 20-meter range, the majority of point clouds in all completed scans are found near the material's surface center. This indicates that the point clouds' reflections from the material borders were slower than the center. This happened because the scan angle of the scanner at the center of the object surface was smaller than the incident angle at the edges, and the large scan angle's intensity was lower than the small ones, while this difference decreases with increasing the range because at large distances the incident angle differences between the center and edges will decrease for the same sample surface. The best-fitting patch for the scanned points is depicted in Figure 20 below, which also notes that, particularly over short distances, the range of points in the surface's center is smaller than that of points on its edges.

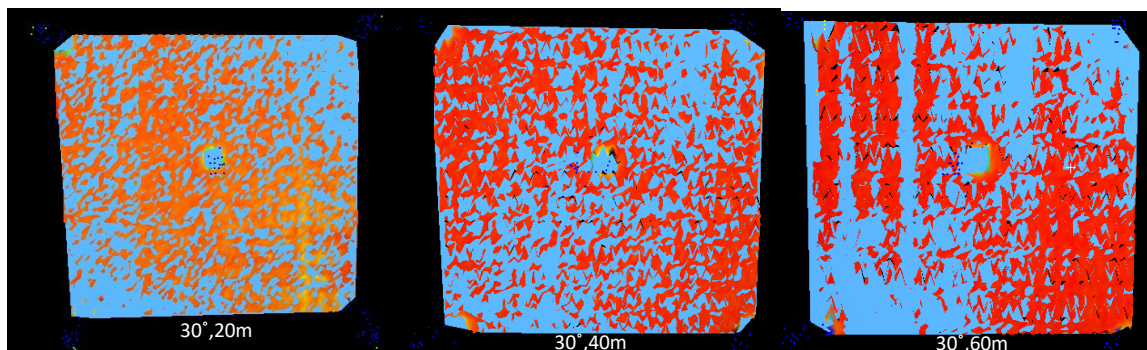


Figure 20: Meshed surface with the best-fit patch of wood sample at 30° scan angle and a range of (20, 40, and 60) m.

The deviation value of the point cloud locations from the best-fitted patch surface has been analyzed, likely for other smooth materials. Thus, at random, 15 points on the surface of the wood image plane and an extra 5 points on the adhesive target sheet have been chosen for each scan incident angle ranging from 0 to 75 degrees and in four different ranges. Figure 21 shows the deviation results for the 30° incident angle in the 20m, 40m, and 60m ranges from left to right.

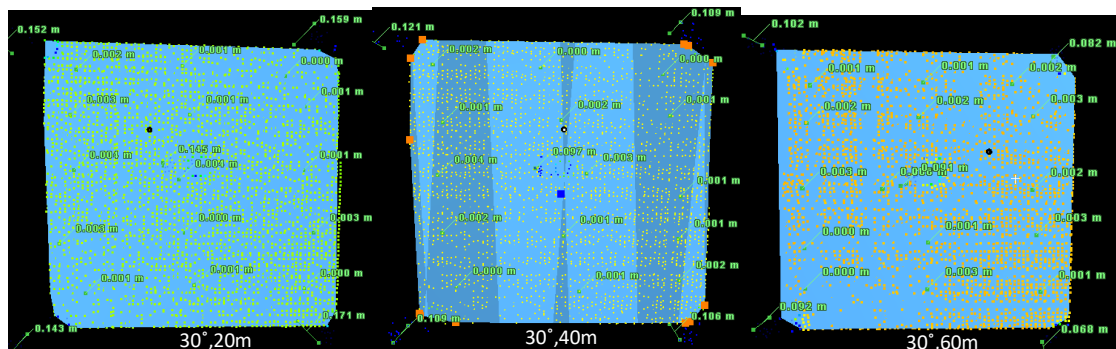


Figure 21: Selected 15 points plus 5 sheet points to examine the difference from the best patch for the wood sample at 30° incident angle and (20, 40, and 60) m ranges.

Table 7: RMSE of 15 point clouds on wood material at 4 ranges and 3 incident angles

Degrees	5m (m)	20m (m)	40m (m)	60m (m)
Wood-0dg.	0.0020	0.0023	0.0027	0.0018
Wood-30dg.	0.0029	0.0017	0.0014	0.0020
Wood-60dg.	0.0009	0.0014	0.0009	0.0009

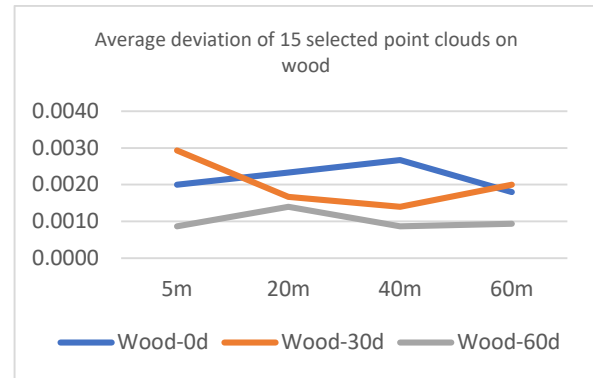


Figure 22: Illustration of the average deviation of 15 point clouds on wood material at 4 ranges and 3 incident angles

The overall average deviation and difference values of the chosen points from the fitted patch are displayed in Figure 22 and Table 7. Minimum deviation values were obtained at a 60° incidence angle of about 1 mm at 40 m and 60 m range, and the maximum deviation emerged at a 30° scanning scan angle around 3 mm at 5 m range. It can be easily seen; the range was not more affected by the rough materials compared with the smooth surfaces.

Additionally, five adhesive total station targets were attached in various spots on the surface prior to scanning. One point cloud per target was chosen in order to determine how far it deviated from the fitted patch. The divergence of the points progressively reduces as the incident angle scan increases from zero to 60°, as indicated in Table 8 and Figure 23. For all ranges, the deviation is approximately 13 to 19 cm when the incident angle is at zero degrees, and it is less than 4 cm for all ranges when the incident angle is at 60 degrees. It indicates that as the incident angle increases when the incident angle approaches 60°, the scanner fails to detect the surface properties of the materials. The variance of these sheet targets on rough material surfaces is smaller than on smooth surface materials when compared to smooth materials. The effect of the distance on the patch deviation at a zero-degree incident angle is greater than that at a non-zero-degree incident angle. When the range increases, the deviation from the patch will decrease. Because the intensity decreases, recognizing and detecting the properties of the surface materials decreases.

Table 8: Target RMSE for 3 different incident angles and 4 different ranges on wood

Degree s	5m (m)	20m (m)	40m (m)	60m (m)
0dg.	0.1570	0.1864	0.1662	0.1276
30dg.	0.1138	0.1540	0.1084	0.0870
60dg.	0.0264	0.0384	0.0244	0.0116

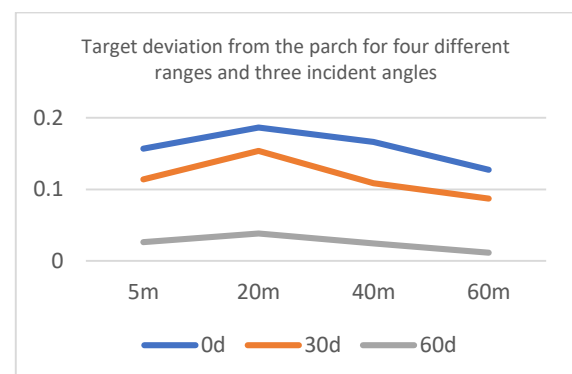


Figure 23: Shows target deviation from the fitted patch for 3 scan angles and 4 ranges on wood material

#### 4.4 Ekoplast Material Scanning Results

Ekoplast is another rough surface material, and it was the last material used for this study. By raising the range and incident angle of the scan, the density of the reflected point clouds decreases,



following a similar process to that used on the materials listed above. The appropriate mesh for the scanned data at 30° and 60° incident angles at 20m, 40m, and 60m range from left to right is shown in Figure 24. This research has consistently shown that the effect of variation in scan angle and distance on rough material surfaces is less than that observed on smooth surface materials, as seen in every figure with incident angles of 60° and a range of 60 m.

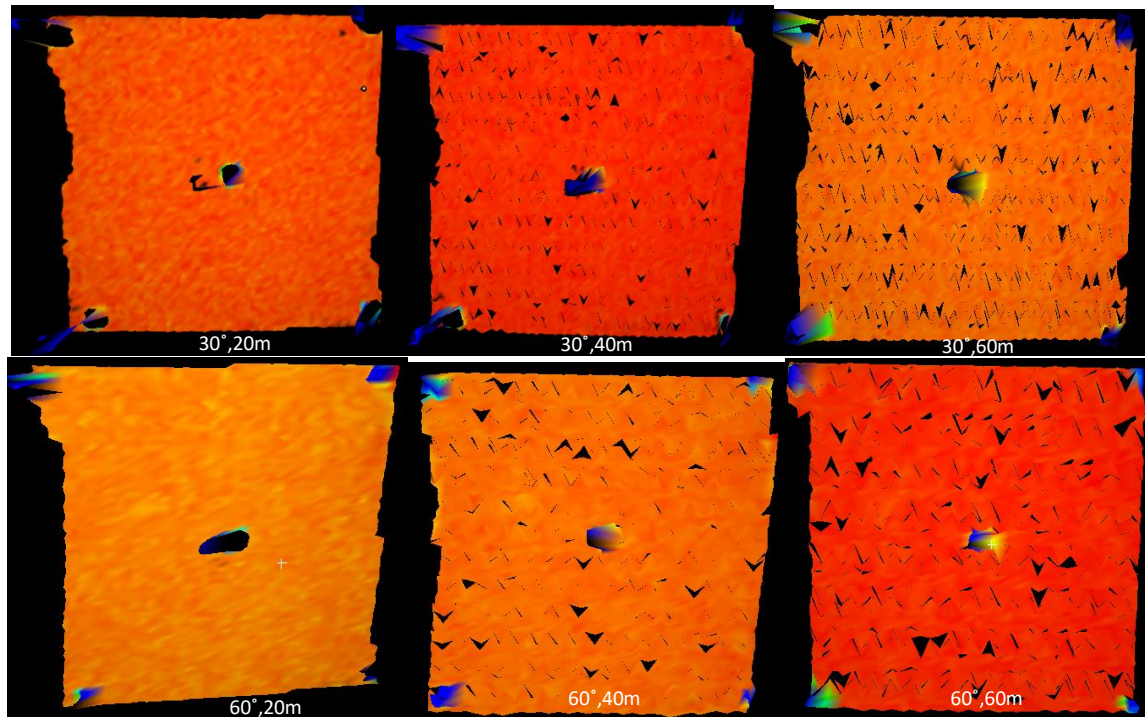


Figure 24: Ekoplast mesh rough surface in (20, 40, and 60) m ranges and at 30° and 60° scan angles

As shown in Figure 25, a best-fit patch was generated for each scan based on the returned points. Based on the range and incident angle of the scans, it is evident that each of the returned points from the material surface of ekoplast has a distinct reflectivity. The point clouds arrive at the scanner ahead of the edges, especially over short distances, at the material surface center because the scan angle is lower there than at the edges and because the intensity from the center is higher than the edges.

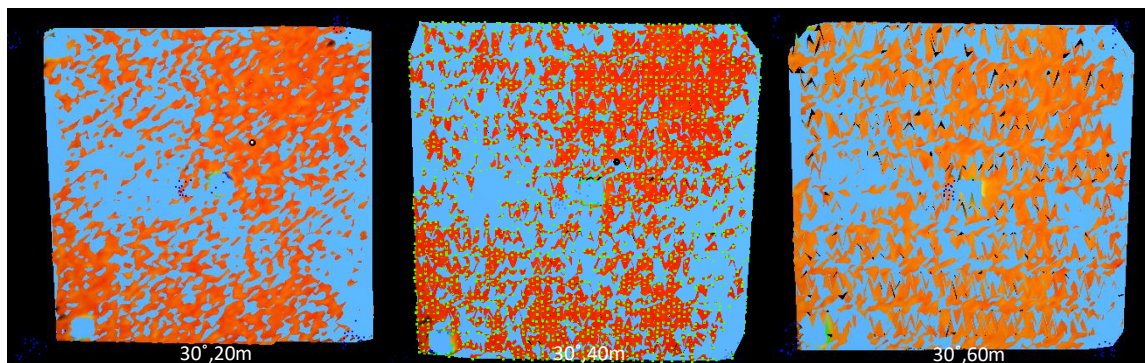


Figure 25: Mesh with best fitted patch for points returned from Ekoplast at 30° scan angle and (20, 40, and 60) m ranges.



To assess this material's response to variations in incidence angle and range. It is calculated to find the deviation values from the patch. Thus, at each incident angle and scan range of zero to seventy-five degrees, randomly chosen 15 points on the surface are performed, with an extra 5-point cloud on the sticky target sheet surface. Figure 26 displays the outcome of the patch deviation.

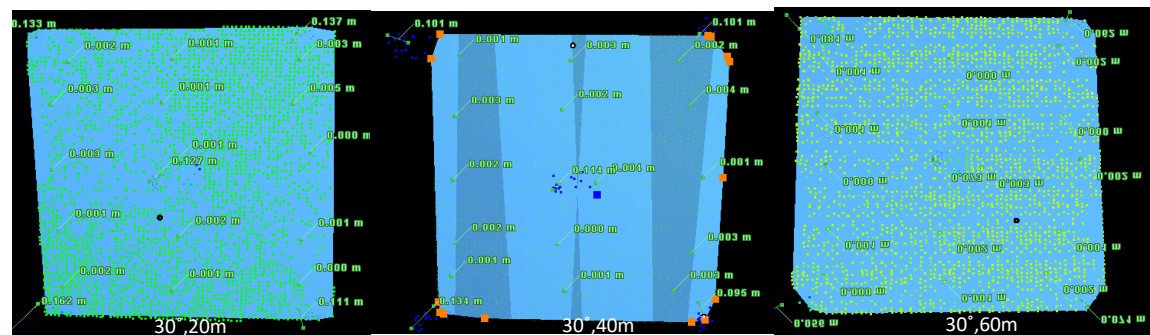


Figure 26: To investigate the deviation from the patch of Ekoplast sample, were selected 15 points plus 5 target points at 30° scan angle and in (20, 40, and 60) m

Table 9: RMSE of 15 point clouds on Ekoplast material in 4 ranges and 3 incident angles

Degrees	5m (m)	20m (m)	40m (m)	60m (m)
Ekoplast-0dg.	0.0019	0.0029	0.0018	0.0022
Ekoplast-30dg.	0.0018	0.0019	0.0021	0.0011
Ekoplast-60dg.	0.0009	0.0013	0.0010	0.0009

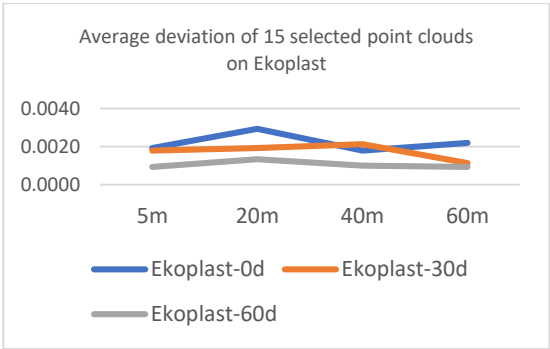


Figure 27: Illustration of the average deviation of 15 points on Ekoplast material in 4 ranges and 3 scan angles

The overall average deviation and difference values of all the chosen point cloud locations from the patch are displayed in Figure 27 and Table 9. The overall deviation decreased at different incident angles; however, the largest deviation showed up at the 0° incident angle of scans, approximately 3 mm in the 20 m range. Because when the incident angle approaches 60 degrees, the scanner fails to detect the surface properties of the materials, and all of them were shown to be similar. The minimum and maximum deviation values at the 60° scan angle are reported in all ranges, ranging from 0.9 to 1.3 mm. The lowest deviation of the smooth materials is about equivalent to the maximum divergence of the reflected points from the fitted patch of this material.

However, five sticky TS targets were also affixed to the surface of the materials in various locations. One point cloud is chosen for each target in order to determine the deviation value from the fitted patch. Therefore, it is evident from Table 10 and Figure 28 that the deviation values of the points decrease across all ranges and at incident angles ranging from zero to 75 degrees. With the exception of the 20-meter range, the deviation values drop to less than 13 mm when the scan angle reaches 60 degrees. This can be confirmed by [3], who found that an increase in the projection angle employed causes a direct drop-in scanning accuracy. When the scan angle is at 0, the deviation and difference value are approximately 12 cm to 18 cm. This difference of zero degrees appeared when adjusting the range. It indicates that as the incident angle increases, the scanner is unable to identify the

characteristics of the materials when the incident angle is close to 60 degrees. The deviation of the targets on materials with rough surfaces is smaller than that of materials with smooth surfaces.

Table 10: Target RMSE for 3 different incident angles and 4 different ranges on Ekoplast

Degrees	5m (m)	20m (m)	40m (m)	60m (m)
0dg.	0.1772	0.1864	0.1238	0.1190
30dg.	0.0980	0.1340	0.1090	0.0686
60dg.	0.0122	0.0340	0.0144	0.0126

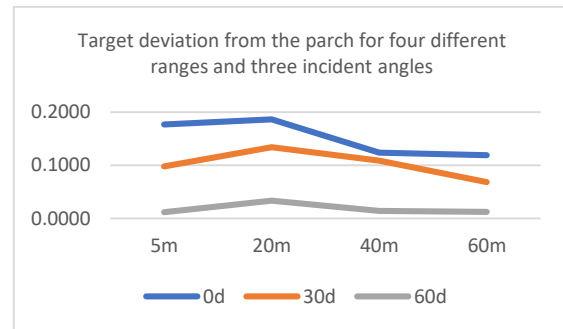


Figure 28: Shows target deviation from the fitted patch for 3 scan angles and 4 ranges on Ekoplast material

## 5. Conclusion

The performance of the scanner in detecting the laser beam duration of the flight and the characteristics of the material's scanned surface are the two key determinants of measurement data accuracy. The actual trials performed in this study have utilized important results regarding surface qualities, the sun's shine, range, and incident angle. These difficulties should be taken into consideration while aiming for extremely high performance in scanner object surface scanning.

First off, Ekoplast and Wood have rough surfaces due to their micro-faced components; hence, they do not record high deviation values at 0° to 75° degrees of scan angle and range; in contrast, glass and steel, which have smooth surfaces, do record big deviation values from 0 to 75°. The maximum relative RMSE for rough materials is less than 3 mm at all distances and incident angles (at wood 30°-5m and ekoplast 0°-20m), while the maximum RMSE for smooth materials glass smooth surface material reaches 8 mm at 30° and 5m range of glass material.

Secondly, the accuracy degree in scanning 3D points varies from one material to another; it depends on the material surface due to differences in its roughness, absorption, transmission, and reflection of the reflected signals. Due to this reason, the data (point clouds) accuracy and quality varied depending on the kind of substance. For example, because steel and glass have different characteristics, the RMSE in glass at a 5 m range and 30° incident angle is 0.79 cm. Conversely, at the same incident angle and range, the RMSE for steel material is 0.21 cm.

Thirdly, a major issue with the accuracy of single-point cloud measuring arises when the scan angle aligns with the angle of sun incidence on a smooth surface, causing the laser beam to return to the scanner on the steel surface more quickly. It occurred at a zero-degree incident angle at a range of five and twenty meters. Likewise, it created an identical issue with the opposite orientation for glass surfaces.

However, the scanner is unable to identify the characteristics of the materials when the incident angle approaches 60° or greater because all of the materials used in the experiment had reflectance and intensity of reflected point clouds that were near one another. As demonstrated for the adhesive total station sheet targets at incident angles of 60° and 75°.

The quality and intensity of the returned laser beam had an impact on the measurement accuracy of point clouds at a range that was greater than zero-degree incident angle. Additionally, the periodical time required to scan an object's surface increases as range increases.

Ultimately, the laser beam takes longer to return to the scanner if the other face of the glass surface material is covered in anything else. This indicates that a portion of the laser signal that passes through the glass and strikes an item behind it does so by returning to the TLS as the secondary return laser signal, and it is demonstrable that the instrument averages the secondary and primary return signals.

The authors plan to conduct a second set of experiments in the future, based on the findings of the current study, to investigate a different factor: the different types of laser beams used by the TLS instruments to scan objects with varying material types.

## 6. Conflict of Interest

There is no conflict of interest for this paper.

## 7. Acknowledgement

This article has been done in partial fulfillment a Ph.D degree in civil engineering/photogrammetry at Salahaddin University-Erbil. Special thanks are directed to the Civil Engineering Department and Geomatics (surveying) staff.

## 8. Authors' contributions

We confirm that all named authors have read and approved the manuscript. We also confirm that each author has made the same contribution to the paper. We further confirm that all authors have approved the order of authors listed in the manuscript.

## References

- [1] Chan TO, Lichti DD. Terrestrial Laser Scanner. 2012;XXXIX(September):169–74.  
<https://doi.org/10.1016/j.isprsjprs.2014.11.003>
- [2] Gumus K, Erkaya H, Soykan M. Investigação referente à repetibilidade do modelo digital de superfície obtido a partir de nuvens de pontos numa barragem abóbada de betão para a monitorização de deformações. Bol Ciencias Geod. 2013;19(2):268–86.  
<https://doi.org/10.1590/S1982-21702013000200007>
- [3] Amer HA, Shaker IF, Ragab A, Abdel-gawad AK, Mogahed Y. Ranges Effect on the Tx5 Laser Scanner Measurements Accuracy. 2019;40–9.
- [4] Tan K, Zhang W, Shen F, Cheng X. Investigation of TLS Intensity Data and Distance Measurement Errors from Target Specular Reflections. 2018;  
<https://doi.org/10.3390/rs10071077>
- [5] Bae K, Lichti DD. On-site self-calibration using planar features for terrestrial laser scanners. ISPRS Work laser scanning. 2007;36(1):14–9.
- [6] Soudarissanane S, Ree J Van. Error budget of terrestrial laser scanning : influence of the incidence angle on the scan quality. 2007;(May 2014) <https://doi.org/10.13140/RG.2.1.1877.6404>.
- [7] Abbas MA, Setan H, Majid Z, Chong AK, Lichti DD, Idris KM. Improvement in accuracy through self-calibration for panoramic scanner. Lect Notes Geoinf Cartogr. 2014;0(March):201–17. [https://doi.org/10.1007/978-3-319-03644-1\\_15](https://doi.org/10.1007/978-3-319-03644-1_15)
- [8] Chan TO, Lichti DD, Belton D. A rigorous cylinder-based self-calibration approach for terrestrial laser scanners. ISPRS J Photogramm Remote Sens [Internet]. 2015;99(June 2018):84–99. Available from: <http://dx.doi.org/10.1016/j.isprsjprs.2014.11.003>
- [9] Amer HA, Shaker IF, Abdel-gawad AK, Ragab A, Mogahed Y. Accuracy Assessment of Laser Scanner under Different Projections Angles. 2018;428–38.
- [10] Lichti DD, Harvey B. the Effects of Reflecting Surface Material Properties on Time-of-Flight

- 
- Laser Scanner Measurements. Geospatial Theory, Process Appl. 2002;(2001).
- [11] Huang X, Zhang Y, Ni B, Li T, Chen K, Zhang W. Boosting Point Clouds Rendering via Radiance Mapping. Proc AAAI Conf Artif Intell. 2023;37(1):953–61.  
<https://doi.org/10.48550/arXiv.2210.15107>
- [12] Julin A, Kurkela M, Rantanen T, Virtanen JP, Maksimainen M, Kukko A, et al. Evaluating the quality of TLS point cloud colorization. Vol. 12, Remote Sensing. 2020.  
<https://doi.org/10.3390/rs12172748>
- [13] Huo L, Liu Y, Yang Y, Zhuang Z, Sun M. Review: Research on product surface quality inspection technology based on 3D point cloud. Adv Mech Eng. 2023;15(3):1–17.  
<https://doi.org/10.1177/16878132231159523>
- [14] Molnár G, Pfeifer N, Ressel C, Dorninger P, Nothegger C. On-the-job range calibration of terrestrial laser scanners with piecewise linear functions. Photogramm Fernerkundung, Geoinf. 2009;2009(1):9–21. <https://doi.org/10.1127/0935-1221/2009/0002>
-